Food and Bioprocess Technology (2022) 16:122–134
https://doi.org/10.1007/s11947-022-02925-x

RESEARCH

Physicochemical Characterization of Texture-Modified Pumpkin by Vacuum Enzyme Impregnation: Textural, Chemical, and Image Analysis

Sergio Hernández[1] · Marta Gallego[1] · Samuel Verdú[1] · José M. Barat[1] · Pau Talens[1] · Raúl Grau[1]

Received: 29 July 2022 / Accepted: 18 October 2022 / Published online: 28 October 2022

Abstract
Texture-modified pumpkin was developed by using vacuum enzyme impregnation to soften texture to tolerable limits for the elderly population with swallowing and chewing difficulties. The impregnation process and macrostructural and microstructural enzyme action were explored by the laser light backscattering imaging technique and a microscopic study by digital image analysis. Texture was analyzed by a compression assay. The effect of enzyme treatment on antioxidant capacity and sugar content was evaluated and compared to the traditional cooking effect. Image analysis data demonstrated the effectiveness of the impregnation process and enzyme action on plant cell walls. Enzyme-treated samples at the end of the process had lower stiffness values with no fracture point, significantly greater antioxidant capacity and significantly lower total and reducing sugars contents than traditionally cooked pumpkins. The results herein obtained demonstrate the capability of using vacuum impregnation treatment with enzymes to soften pumpkins and their positive effects on antioxidant capacity and sugar content to develop safe and sensory-accepted texture-modified products for specific elderly populations.

Keywords *Cucurbita moschata* · Vacuum impregnation · Elderly population · Texture-modified foods · Antioxidant capacity · Sugars

Introduction

Declining birth rates and longer average life expectancy have led to a change in the age structure population and generated rapid aging (Aguilera & Park, 2016). United Nations (2020) estimations predict an increase from 9.3 to 16% in the population aged over 65 years in 2050, which means that there will be 1.5 billion people within this age range. Hence ensuring seniors' health, well-being, and quality of life has become a priority and crucial aspect.

Elderly people can have chewing and swallowing difficulties because of many disorders, such as sarcopenia (loss of muscle mass), osteoporosis (decline in bone mass and strength), xerostomia (reduced salivation), loss of appetite or dental pieces, dysphagia (difficulties with forming safe-to-swallow boluses), and gastrointestinal alterations. (Aguilera & Park, 2016; Gallego et al., 2022). These dysfunctions can also imply unbalanced diets with vitamin or mineral deficiencies and malnutrition because these people are prone to remove from their diet those foods that cause them discomfort, such as some vegetables that are difficult to chew, swallow, or prepare (Roininen et al., 2004). One way to adapt the texture of vegetables by increasing their softening is by overcooking, which leads to loss of vitamins, minerals, and antioxidant compounds and an increase in sugar content (Kao et al., 2014; Lešková et al., 2006; Miglio et al., 2008; Singh et al., 2020). Moreover, in some cases, it is not even possible to achieve suitable textures by overcooking because some vegetables, such as tubers, can still imply certain hardness or have a heterogeneous texture. In the end, they have to be thickened as purée after being crushed, which reduces their appetizing nature and food volume intake and may, therefore, also increase malnutrition.

In this sense, texture-modified (TM) foods are usually prescribed to guarantee efficient and safe intake in older people (Cichero et al., 2013). The problem is that these TM foods normally come as creams, soups, purées, or

✉ Sergio Hernández
serhert1@upv.es

[1] Departamento Tecnología de Alimentos, Universitat Politècnica de València, Camino de Vera s/n, 46022 5 Valencia, Spain

mousse that consumers might detest (Park & Lee, 2020). So developing homogeneous texture food usually identified as "solid" (e.g., pumpkin, carrot, meat), but is very soft, and can even be immersed in thickened soup with the same texture, might be a solution.

In this way, 3D printing has emerged as an innovative alternative to developing TM food improving its appetizing (Gallego et al., 2022; Wilson et al., 2020). This technique has some advantages such as allowing the development of foods with complex and attractive shapes with personalized nutrition and some disadvantages such as the low production volume and low printing speed (Sun et al., 2015; Tomašević et al., 2021).

Another effectively applied alternative is the softening by enzyme treatment and using vacuum impregnation (Shibata et al., 2010). This technique permits the rapid impregnation of enzymes in a foodstuff matrix (Nakatsu et al., 2012; Yang et al., 2017), which can create TM foods without interfering with their original shape, which results in appetizing diets for the elderly population. Many advances have been made in vegetables, which are developed by applying pectinase enzymes through impregnation to hydrolyze pectin from plant cell walls (Eom et al., 2018; Sakamoto et al., 2006), but very little is known about the effect on the bioaccessibility of polysaccharides and their molecular weight. Although this technique has been applied to several vegetables, such as carrots, burdock roots, lotus rhizomes, and bamboo shoots, among others (Eom et al., 2018; Nakatsu et al., 2012), we found no studies on pumpkin. This fruit has many human health benefits because it is a source of pectin, carbohydrates, vitamins, minerals, and phenolic compounds (Bai et al., 2020; Li et al., 2021; Paciulli et al., 2019; Phuhongsung et al., 2020). Pumpkin has been related to several bioactive functions, including antidiabetic, antihypercholesterolemic, antihypertensive, or antioxidant activities (Zhou et al., 2014). Antioxidant compounds are highly recommended for the elderly population because they counteract oxidative stress, and they have positive effects on dementia and cognition disorders and pneumonia, among others (Achir et al., 2016; Lee et al., 2020; Wichansawakun et al., 2022). These aspects make pumpkin a very suitable food for the elderly population. Thus studying the pumpkin enzyme treatment to obtain a TM food and comparing the procedure effects on two components that are usually altered by overcooking, followed by grinding and thickening, such as antioxidant activity and sugar content, are important aspects for its development.

This paper aimed to soften pumpkins by vacuum enzyme impregnation treatment to create safe TM foods for the elderly population. Imaging and texture analyses were used to study the softening process. Antioxidant activity and sugar content were evaluated to compare the enzyme treatment effects throughout the process to those of traditional cooking.

Materials and Methods

Materials and Reagents

Pumpkins (*Cucurbita moschata*), purchased from a local supermarket (Valencia, Spain), were cut into cylinders (2 cm diameter × 2 cm high) using a slice cutter (Slice Cutter MS 4570, Orbegozo, Murcia, Spain) and a metallic core bore. Enozym Vintage, containing polygalacturonase (PG), pectin methylesterase (PME), and pectin lyase (PL) enzymes, was provided from Agrovin S.A. (Ciudad Real, Spain). Reagents 2,2-diphenyl-1-picrylhydrazyl (DPPH), butylated hydroxytoluene (BHT), potassium persulfate, and 2,2′-azino-bis (3-ethylbenzothiazoline-6-sulfonic acid) diammonium salt (ABTS), 3,5-dinitrosalicylic acid, D-glucose, carbazole, and D-(+)-galacturonic acid monohydrate were purchased from Sigma-Aldrich, Co. (St. Louis, MO, USA). Phenol was purchased from Labbox Labware, S.L. (Premiá de Dalt, Barcelona, Spain), Trolox was from Acros Organics (Fair Lawn, NJ, USA), and ascorbic acid and potassium sodium tartrate tetrahydrate were bought from Scharlau Chemie, S.A. (Sentmenat, Barcelona, Spain).

Experimental Procedure

The experiment was performed in three stages (Fig. 1). Enzyme impregnation effectiveness and inactivation processes were explored in the first stage. To this end, a laser light backscattering technique and a microscopic assay, via digital image analysis, were used. Three different sample types were evaluated: (a) impregnated with enzymes to evaluate their effect on pumpkin structure; (b) impregnated with inactivated enzymes to assess inactivation treatment efficiency; and (c) impregnated with water to evaluate the impregnation process. To assess the inactivation treatment, samples were impregnated with the previously inactivated enzymes. For this purpose, steaming time was reduced from 5 min (time obtained in preliminary heat penetration studies in pumpkin when 85 °C at the center of samples was recorded for more than 2 min (data not shown)) to 2 min for the enzyme solution. Enzymes were impregnated after their inactivation because heat inactivation treatment brings about changes in samples' texture, which are captured by image techniques.

In the second stage, the goal was to achieve a pumpkin with maximum softening while maintaining its original appearance to obtain a product with a texture that adapts to the elderly population. For this purpose, a compression test was performed on the raw (R), control (C), and

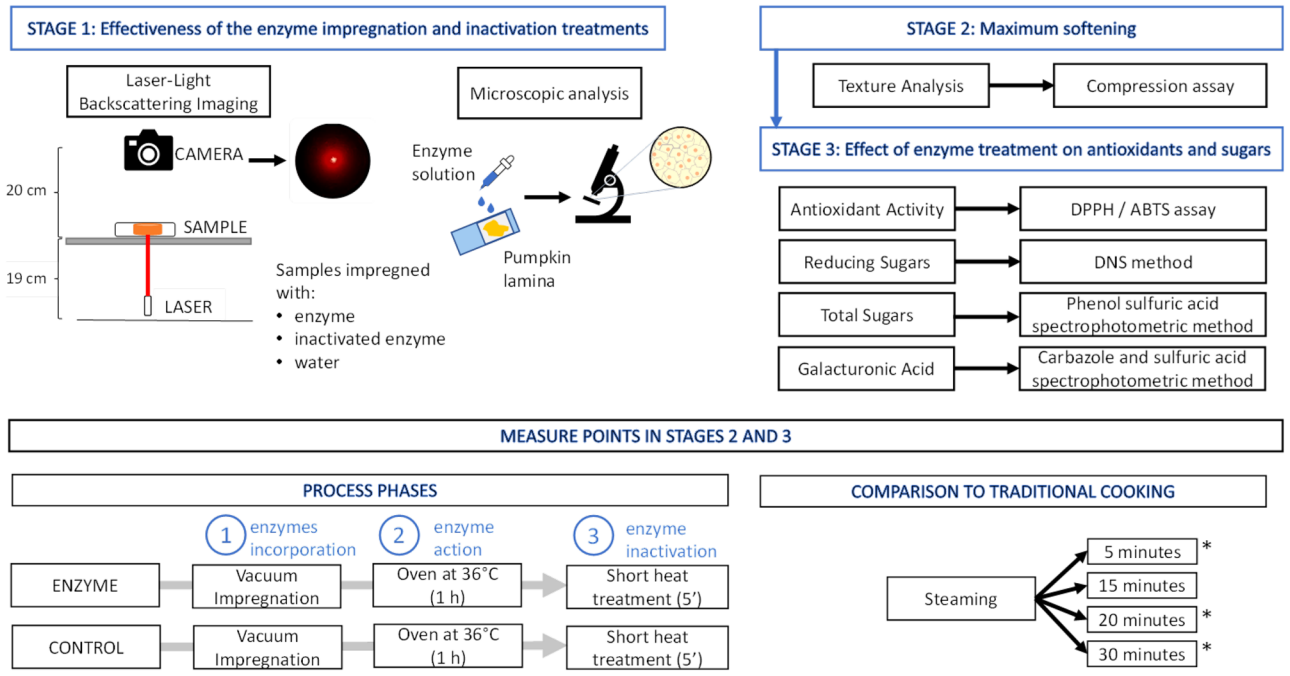

Fig. 1 Scheme of the experimental procedure. *These conditions were tested only in stage 2 (texture analysis)

enzyme-treated (E) samples in three process phases (1, vacuum impregnation treatment to incorporate enzymes; 2, oven for enzyme action; 3, short heat treatment for enzyme inactivation). In parallel, another group of samples was traditionally cooked by steaming treatment for 5, 15, 20, and 30 min (S5, S15, S20, and S30, respectively) to evaluate the cooking time variable and to compare the effect of enzyme treatment to that of traditional cooking on texture properties.

In the third stage, the effect of enzyme treatment on antioxidant activity and the total and reducing sugar contents of the TM pumpkin were studied. These analyses were carried out at the same points as in the second stage, except for the cooked samples for which the most appropriate steaming time was chosen. The galacturonic (GalA) acid content of the enzyme-treated samples was measured at the end of the process (E3) and in the traditionally cooked pumpkins (S15) to evaluate the degree of pectin esterification (DE).

Treatment

The overall process was similar to that used by Nakatsu et al. (2012) and Park and Lee (2020) with slight modifications. Samples were immersed in 400 mL solution containing 0.5% of the enzyme mixture containing PG, PME, and PL activities. Citric acid (8.3 mM) was added to reach pH 4 and to improve enzyme action. Then the immersed samples were placed in a vacuum chamber, and vacuum pulse was applied. Pressure conditions reached 85 kPa and were kept for 5 min. To complete impregnation, samples were returned to atmospheric pressure in 1.5 min. After vacuum treatment, samples were removed from the enzyme solution and placed inside an oven at 36 °C, where they were left for 1 h for enzyme action. Then enzymes were inactivated by short heat treatment based on 5 min applying steam. In parallel to this, other samples were cooked by steaming for 5, 15, 20, and 30 min.

Image Analysis

Laser-Light Backscattering Imaging

The laser-light backscattering imaging technique (LLBI) was used to explore the enzyme impregnation process induced by vacuum and to verify the effectiveness of the selected heat treatment conditions to inactivate enzymes. This technique has been effectively applied to model different processes in the agri-food sector (Adebayo et al., 2016) and to characterize enzyme action in several food matrices (Grau et al., 2021; Verdú et al., 2021). Image system acquisition with a red laser diode and a webcam (HD cam C615) in a dark chamber was used to record the diffraction patterns (Fig. 1, stage 1).

Samples were impregnated with enzymes, water (control), and inactivated enzymes following the previous experimental procedure. After impregnation, samples were removed from the solution and placed inside the chamber for the imaging analysis at room temperature. A redpoint light from a laser diode (650 nm, 50 mW) was perpendicularly

placed 19 cm under the samples to form diffraction patterns on them. These patterns were video-recorded for 5 h.

Microscopic Analysis

A microscopic study was carried out to explore the microstructure evolution of the enzyme-treated samples. Pumpkin tissue laminas were cut using a microtome (Microtome MT.5503, EUROMEX Microscopen B.V, the Netherlands). Cut sections were impregnated by 0.1 mL of enzyme solution. Samples were covered with a coverslip to avoid dehydration. RGB images at the 2048 × 1536 resolution were taken every 5 min with a CMOS camera Moticam 3 + (Motic, Hong Kong, China) connected to a BA310E microscope (Motic, Hong Kong) at 40 × magnification.

Image Processing

The videos obtained from LLBI were segmented on the RGB images (RGB stack, S_{RGB}). These images and the microscopy RGB images were converted into grayscale (8 bits) to simplify the intensity information (gray stack, S_g). Change zones were identified by subtracting the first image from the stack of images. Thus, a difference stack was obtained (S_d). By this method, pixels' areas were attributed to changes in transmittance as a result of structural changes. With the laser results, the area of change (in pixel units) per minute was plotted to describe diffraction pattern evolution for the active and inactivated enzymes and the control samples. For the microscopic data, histograms of frequency (number of pixels) per pixel gray value were calculated and plotted for images at times 0, 25, and 150 min and for the difference between the final time (150 min) and the initial time (0 min) (S_d). This calculation was used to detect the gray value threshold with changes and to determine the location of the pixels that changed. Next the gray values between 16 and 80 were selected, and S_d was thresholded to emphasize changes and to identify zones with microstructural changes. The image analysis was carried out by the Fiji image software (Fuentes et al., 2022). Five replicates per group were taken.

Texture

Texture was characterized by a compression test (Andersson et al., 2022) carried out with a TA-TX2 texture analyzer (Stable Micro Systems, Surrey, UK), equipped with a 25 kg load cell. This study intended to characterize the raw (R), control (C), and enzyme-treated (E) samples in the three process phases, as well as samples steamed for 5, 15, 20, and 30 min (S5, S15, S20 and S30, respectively) (Fig. 1). Samples were compressed to 50% deformation via a cylindrical disc (75 mm diameter). The test speed was 1.00 mm/s. The fracture point (N) and Young's modulus (kPa), which was calculated from the ratio between the true stress and true strain from the linear region of the compression curves according to Eq. (1) as described by Andersson et al. (2022), were analyzed for all the samples.

$$Young's\ modulus = \frac{\frac{F(t) \times (h_i - \Delta h(t))}{\pi \times r_i^2 \times h_i}}{\ln\left(\frac{h_i}{h_i - \Delta h(t)}\right)} \quad (1)$$

where $F(t)$ is the force, h_i is the initial height, $\Delta h(t)$ is the change in height, and r_i^2 is the sample's initial radius. Tests were performed on five replicates per sample.

Sample Preparation

The extraction procedure was based on the method described by Lyu et al. (2021) with slight modifications. Briefly, 10 g of each sample were mixed with 10 mL of methanol (80%) or distilled water for the antioxidant or sugar determinations (total and reducing sugars and GalA content), respectively. Solutions were centrifuged at 10,000 rpm and 4 °C for 15 min, and supernatants were collected. Extracts were kept frozen (−20 °C) until analyzed. Antioxidant activity was determined by the 1,1-diphenyl-2-picrylhydrazyl (DPPH) and 2,2′-azinobis-(3-ethylbenzthiazoline-6-sulphonate (ABTS) methods. An UV–visible spectrophotometer (Helios Zeta, Thermo Scientific, UK) was used to measure absorbance, and analyses were performed in triplicate.

Antioxidant Activity

DPPH Assay

DPPH radical scavenging activities of the sample were determined as described by Zhou et al. (2014) with slight modifications. First, 200 µL of sample extract was mixed with 1000 µL of methanol and 250 µL of a methanolic solution of DPPH (0.02%). Absorbance was measured at 517 nm after a dark incubation time for 60 min at room temperature. Calibration curves were prepared using Trolox (0–200 µmol/L), and methanol (80%) was employed as a blank and BHT as a positive control. The results were expressed as micromoles of Trolox equivalent antioxidant capacity (TEAC) per gram of sample.

ABTS Assay

ABTS radical scavenging activities of the samples were determined according to the method reported by Gallego et al. (2021). ABTS radical cation was formed by dissolving 7 mM of ABTS solution in 2.45 mM sodium persulfate solution and incubating in dark for 14–16 h at room

temperature. This solution was diluted with phosphate buffer saline (PBS) (pH 7.4) up to an absorbance of 0.7 at 734 nm. Then, 10 µL of sample and 990 µL of ABTS solution were mixed, and absorbance was measured at 734 nm after 6 min of incubation. Calibration curves were prepared with Trolox (0.075–2 mM), PBS was used as a blank, and ascorbic acid was the positive control. The results were expressed as nanomoles of TEAC per gram of sample.

Total Sugars, Reducing Sugars, and Galacturonic Acid

Total Sugars

Total sugar concentration was measured by the phenol–sulfuric acid method described by Dubois et al. (1956) with slight modifications. Briefly, 0.2 mL of samples and 1 mL of sulfuric acid were mixed rapidly in Pyrex tubes. Afterward, 0.2 mL of phenol (5%) was added, and tubes were incubated at room temperature for 10 min. Then tubes were mixed and incubated for 15 min, and absorbance was measured at 490 nm. Calibration curves were prepared using D-glucose (0–100 µg/mL) and distilled water was employed as a blank. The results were expressed as mg of glucose per gram of sample.

Reducing Sugars

The reducing sugar concentration was measured by the dinitrosalicylic (DNS) method described by Gwala et al. (2019) with slight modifications. DNS solution was prepared by mixing 1 g of 3,5-dinitrosalicylic acid, 30 g of potassium tartrate tetrahydrate, and 20 mL of NaOH to be diluted up to 100 mL with distilled water. Then 500 µL of DNS solution and 50 µL of sample were mixed in Pyrex tubes and boiled for 5 min in a water bath. Next tubes were placed in an ice bath, and 4.5 mL of distilled water were added. The absorbance of samples was measured at 540 nm. Calibration curves were prepared using D-glucose (0.5–14 mg/mL), and distilled water was employed as a blank. The results were expressed as mg of glucose per gram of sample.

Galacturonic Acid (GalA)

GalA content was determined by the sulfuric acid-carbazole method described by Cesaretti et al. (2003) with slight modifications. Briefly, 0.15 mL of samples and 0.6 mL of 25 mm sodium tetraborate in sulfuric acid were mixed in Pyrex tubes. Then tubes were heated for 10 min at 100 °C in a water bath. Next tubes were cooled at room temperature for 15 min, and 0.15 ml of 0.125% carbazole in ethanol was added. The mixture was heated again at 100 °C for 10 min and then cooled for 15 min before measuring absorbance at 550 nm. Calibration curves were prepared using D-(+)-GalA (0—1 mg/mL), and distilled water was employed as a blank. The results were expressed as mg of GalA per gram of sample.

Statistical Analysis

The results are reported as mean values with standard deviation. Variance was studied by simple ANOVA with a 95% confidence level. In those cases for which the effect was significant, the means were compared by Fisher's least significant difference (LSD) procedure. The employed software was Statgraphics Centurion XVII.II, version 17.2.04.

Results and Discussion

Stage 1: Effectiveness of the Enzyme Impregnation and Inactivation Treatments

The effectiveness of the impregnation process and the inactivation treatment of the enzymes by short heat treatment were evaluated by the LLBI technique. Figure 2A shows the area of change compared to time 0 according to the time for samples to be impregnated with enzymes, inactivated enzymes, and water.

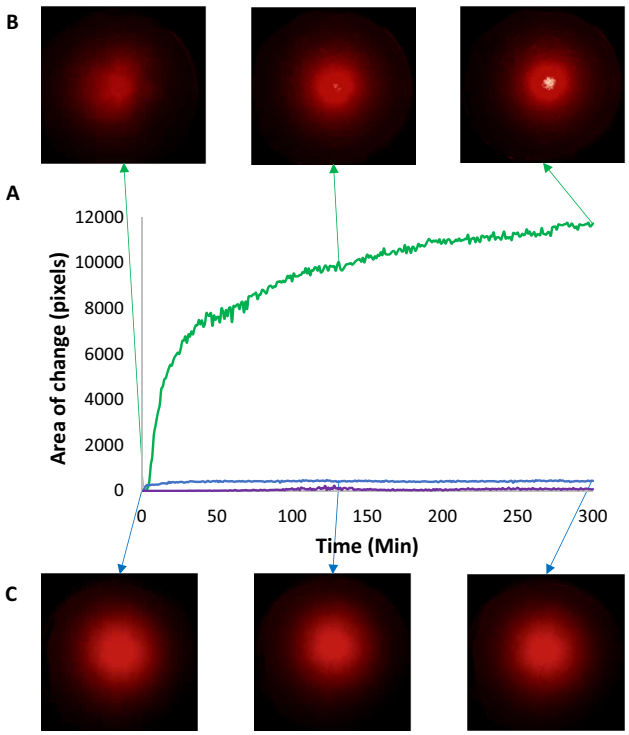

Fig. 2 Area of change (pixels unit) evolution according to time for the enzyme-treated (green line), inactivated enzymes (purple line), and the control samples (impregnated with water) (blue line) (**A**) with their respective diffraction patterns at RGB model for samples treated with enzymes (**B**) and control (**C**)

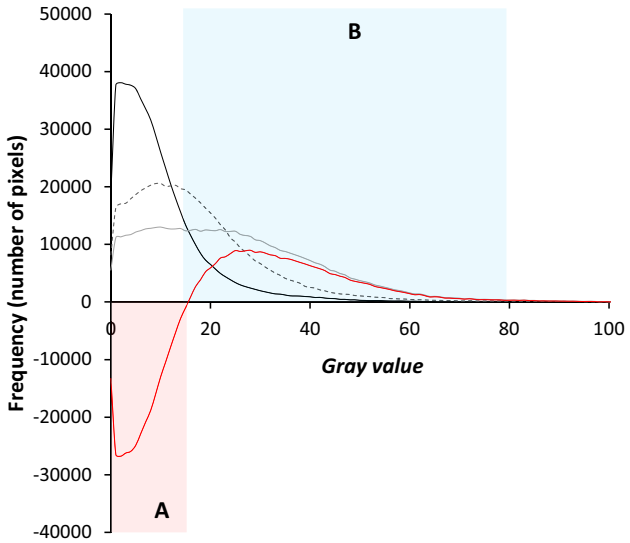

Fig. 3 Frequency histograms of the gray value for times 0 min (black line), 25 min (gray dashed line), and 150 min (gray continuous line) and the subtraction of the final image (150 min) minus the initial image (0 min) (red line)

Changes generated on the samples impregnated with inactivated enzymes and water (control) were insignificant compared to those of the enzyme-treated samples, which underwent notorious change in the area of their pixels (Fig. 2A). Lack of changes in the samples treated with inactivated enzymes justified the efficiency of the short heat treatment on enzyme inactivation. This fact informed about the kinetics of enzymes' action and their speed at room temperature, which produced most of the structural changes within the first 60 min (70% of change) and showed an almost unchanged phase after a couple of hours. Having explored the evolution of the area of change, the direction of changes was evaluated. These changes in the diffraction patterns took place due to an increase in the gray value, and the pixel value shifted to whiter values, as shown by the images in Fig. 2B. Between 4 and 5 h of enzyme action, the center of the diffraction pattern reached a maximum intensity peak, which is commonly known as Airy disk (Verdú et al., 2019). This increase in the pixel value was not observed in the diffraction pattern of the control samples (Fig. 2C). This behavior of the enzyme-treated samples was probably due to increased transmittance as a consequence of cell walls breaking down. To obtain more information about this phenomenon and to specify the microstructural origin, an analysis of microscopic images was also carried out. For this purpose, the distribution of the value of pixels was explored by histograms of the frequency gray value of S_d (Fig. 3) to find out the location of the pixels that changed and, hence, the changing zones of pumpkin cell tissues (Fig. 4).

As the number of pixels in the image was always the same, the area under the curve informed about the distribution of the pixel values in each image of the stack. As seen in Fig. 3, the pixel values shifted to white (higher) values as in laser results, and their transmittance increased. Thus in the image at 150 min (gray continuous line), a shifting of their area in relation to the image at time 0 (black line) occurred. To obtain the location in the image of the pixels that changed, we made an attempt to find out their gray value. To do so, the frequency of the pixel values in the initial image (0 min) was subtracted from those from the final image (150 min) (red line). This line denoted the threshold of the pixel values with the changed regions because it represents the point at which the increment in changes became positive (B square in Fig. 3). For this purpose, the threshold between 16 and 80 Gy values was selected. Next S_d was thresholded by applying this selection (Fig. 4B). This image operation highlighted the zones with the most changes. Thus, the white zones in the images of Fig. 4B were the zones with more structural changes and corresponded to plant cell walls. These results demonstrated the enzyme action by hydrolyzing pectin, which is the main plant cell

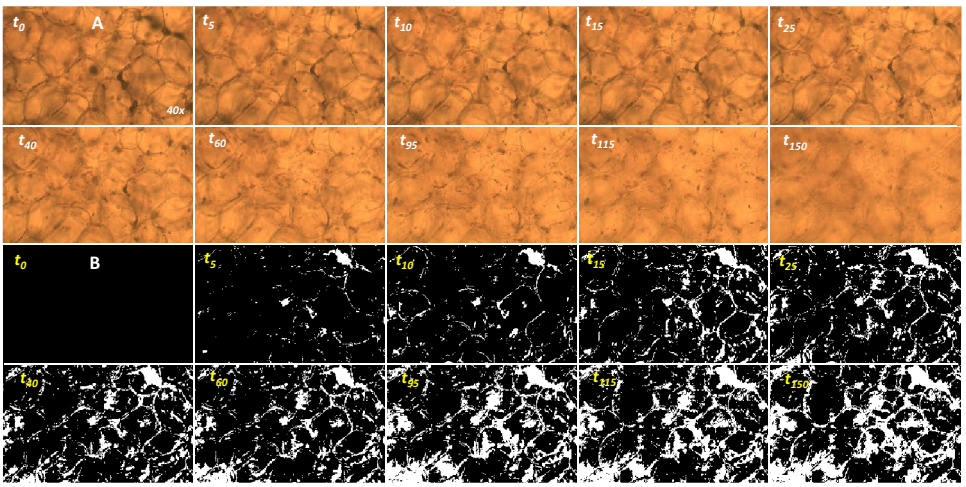

Fig. 4 Microscopic images taken during enzyme action corresponding to S_{RGB} (**A**) and S_d (**B**)

wall component (around 35%). Furthermore, pectin forms, together with hemicellulose, a matrix in which cellulose microfibers are embedded, play a crucial role in structural and textural aspects (Bermejo-Prada et al., 2014). This causes loss of cell turgor and compaction, and, hence, the light path increases. This was observed by the LLBI and microscopic studies.

Stage 2: Maximum Softening Studies

The fracture point (N) and Young's modulus (kPa) of the raw (R), control (C), and enzyme-treated (E) pumpkins in the different process phases (1: vacuum impregnation treatment; 2: enzyme action time; 3: enzyme inactivation) and of the samples traditionally cooked by steaming for 5, 15, 20, and 30 min (S) are represented in Fig. 5.

Fracture point indicates the sample's strength, whereas Young's modulus is related to the stiffness of vegetables and can be obtained from the slope of the linear region of compression curves (Andersson et al., 2022; Medina-Torres et al., 2009). These parameters are related, but provide different and complementary information. Furthermore, Young's modulus permits all the samples to be compared, and not only those with fracture as the first mentioned parameter.

As Fig. 5A illustrates, the R samples were those with a higher fracture point. This group of samples, together with C1 and C2, also had the highest Young's modulus values (Fig. 5B). The fracture point of the C samples decreased slightly during vacuum treatment upon water solution and enzyme action (phases 1 and 2), while Young's modulus remained stable at the similar high values to R, which indicates greater stiffness. The inactivation treatment (phase 3) led to a drastic significant reduction in both parameters, although their values were still high (28.6 ± 10.5 N for fracture point and 554.9 ± 177.4 kPa for Young's modulus). On other hand, the values of both parameters lowered for the S samples compared to the R samples. The decrease in the Young's modulus values by steaming has also been reported by Andersson et al. (2022). Among S samples, S5 showed the harder strength and stiffness level, whereas non-significant differences were found from 15 min of steaming. S15 obtained a fracture point of 6.6 ± 2.6 N, with 309.8 ± 69.7 kPa for Young's modulus, and was the steaming time chosen for the rest of the study, similarly to Mashiane et al. (2021) and Dini et al. (2013).

The fracture point of the E1 samples considerably decreased (69.0 ± 26.5 N) compared to the R samples, whereas E2 and E3 did not suffer from fracture during compression. This is probably due to an important reduction of its strength as a result of cell walls breaking down commented previously. At this point, the pumpkin has a gel-like appearance as its structure resembles a solid. This denotes a more homogeneous texture, which would be an advantage for foods prepared for the elderly population. Furthermore, the Young's modulus values of the E samples significantly

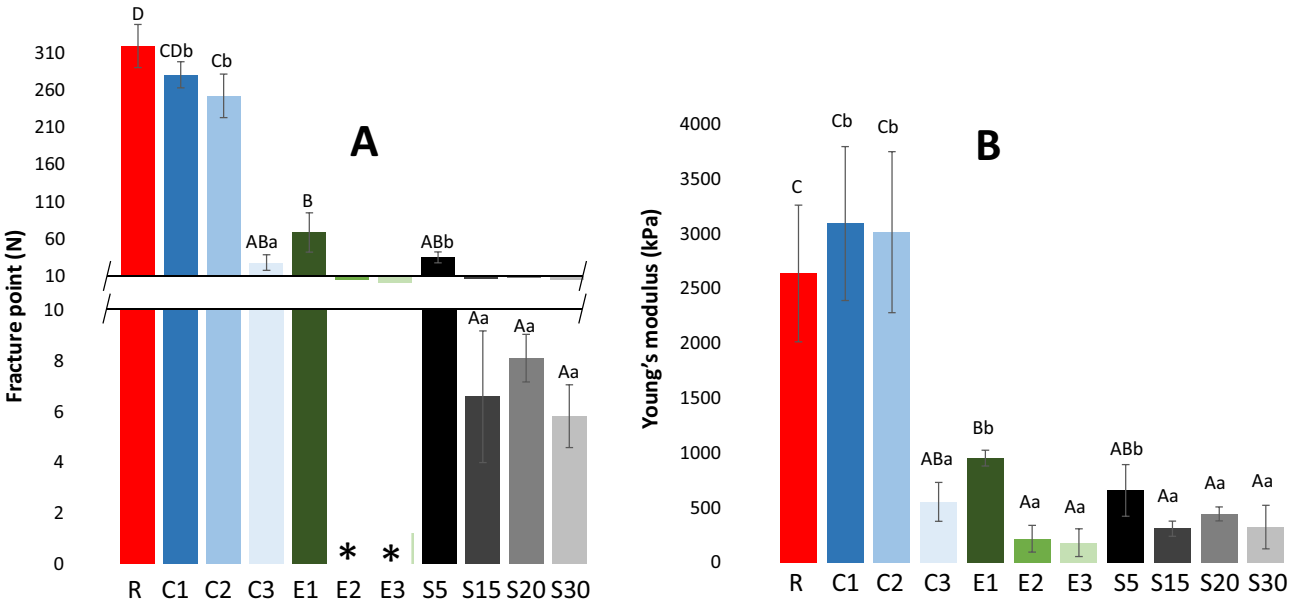

Fig. 5 The fracture point (N) (**A**) and Young's modulus (kPa) (**B**) values of the raw (red bar), control (blue bars), and enzyme-treated (green bars) samples after the three process phases (1, vacuum impregnation; 2, enzyme action time; 3, enzyme inactivation) and the traditionally cooked samples (gray bars) at the different cooking times (5, 15, 20, 30 min) with standard deviation. Uppercase letters indicate significant differences among all the samples. Lowercase letters denote significant differences between the distinct treatments (control, enzyme, steaming). Asterisks mark the samples with no fracture point

lowered during the process, and E2 and E3 presented the lowest Young's modulus values (217.9 ± 122.6 kPa and 181.7 ± 126.0 kPa, respectively) and were, hence, the samples with the least stiffness. Compared to S15, the Young's modulus value of E3 was 41% lower, which implies a significant reduction in stiffness.

Figure 6A shows representative true stress-true strain curves of E3 compared to the S samples. The shape of these curves provided information about samples' textural homogeneity and stiffness. The true stress scores for S5 drastically dropped when the disc passed external regions and began to compress internal regions (at around 5 s). This behavior was probably due to a fracture point and lack of cooking, which provoked a heterogeneous texture that could pose a risk for the elderly population (Alcalde et al., 2020). As steaming time increased, pumpkin textures became more homogeneous, characterized by more constant true stress-true strain curves with lower true stress values. Yet not even 30 min of steaming avoided fracture. The red arrows in Fig. 6A and B indicate the fracture point and, hence, the regions with a heterogeneous texture of these samples. However, E3 no longer presented a fracture point (blue arrows), which resulted in a totally homogeneous texture. Hence given these samples' greater texture homogeneity because a fracture point was lacking and their lesser stiffness would make the enzyme-treated samples a suitable TM food for the elderly.

Stage 3: Effect of Enzyme Treatment on the Antioxidant Activity and Sugar Content of TM Pumpkins

Having selected 15 min of steaming as the traditional cooking condition based on previous texture studies, the antioxidant activity and sugar content of the raw (R), control (C), enzyme-treated (E), and traditionally cooked (S15) samples were analyzed.

Antioxidant Activity

The antioxidant activity of pumpkins is related to phenolic compounds, polysaccharides, ascorbic acid, flavonoids, and carotenoids, among others (Li et al., 2021; Su et al., 2019; Zhou et al., 2017) and was determined by the DPPH and ABTS methods because no single validated antioxidant determination method exists (Huang et al., 2005; Longato et al., 2017). Both assays are based on electron-transfer (ET) reactions, but can also act in hydrogen atom transfer (HAT) reactions (Prior et al., 2005). The antioxidant activity of pumpkins after different cooking methods has been widely studied (Andersson et al., 2022; Ribeiro et al., 2015). However, there are no studies that have evaluated the antioxidant activity of pumpkins softened by vacuum enzyme impregnation treatments.

The DPPH radical scavenging assay showed that S15 had the least antioxidant activity (3.9 ± 0.1 μmol TEAC/g) (Fig. 7A). This could be due to extensive thermal treatment, which can deteriorate the antioxidant compounds present in pumpkins. These results fall in line with those reported by Kao et al. (2014), who described diminished antioxidant capacity of vegetables due to the long-term cooking effect associated with a decline in phenolic compounds. Interestingly, short heat treatment (5 min) significantly increased the antioxidant capacity for C3 and obtained the highest values (13.7 ± 0.1 μmol TEAC/g). This increase can be provoked by the breakdown of compounds like phenols or by the production of secondary

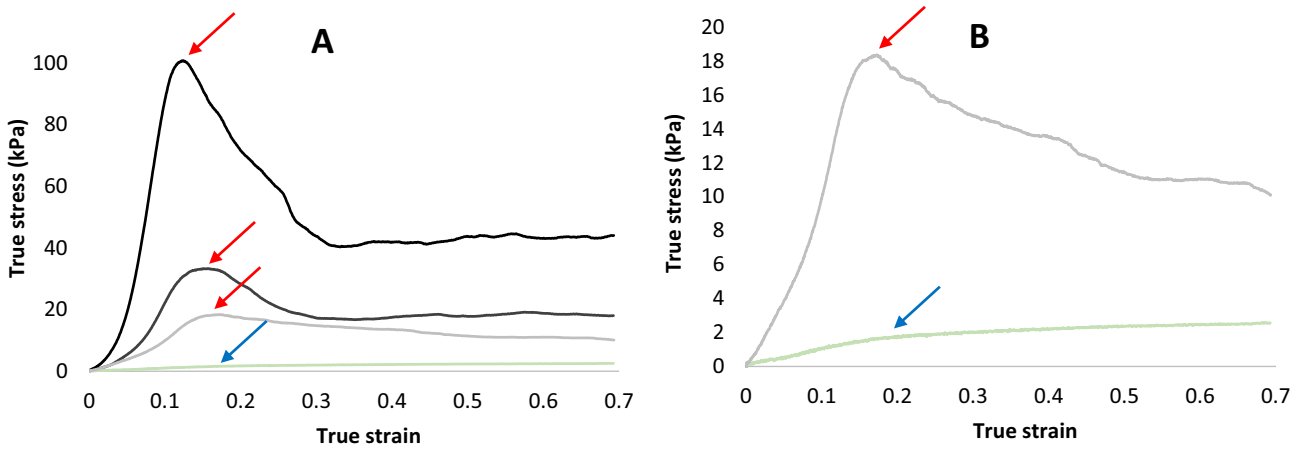

Fig. 6 Representative true stress-true strain curves of the samples steamed for 5 (S5, black line), 15 (S15, dark gray line), and 30 (S30, light gray line) min, along with the enzyme-treated sample, at the end of the process (E3, pale green line) (**A**). Representative true stress-true strain curves of S30 (light gray line) and E3 (pale green line) on a larger scale (**B**). Red arrows indicate the fracture point; blue arrows denote no fracture

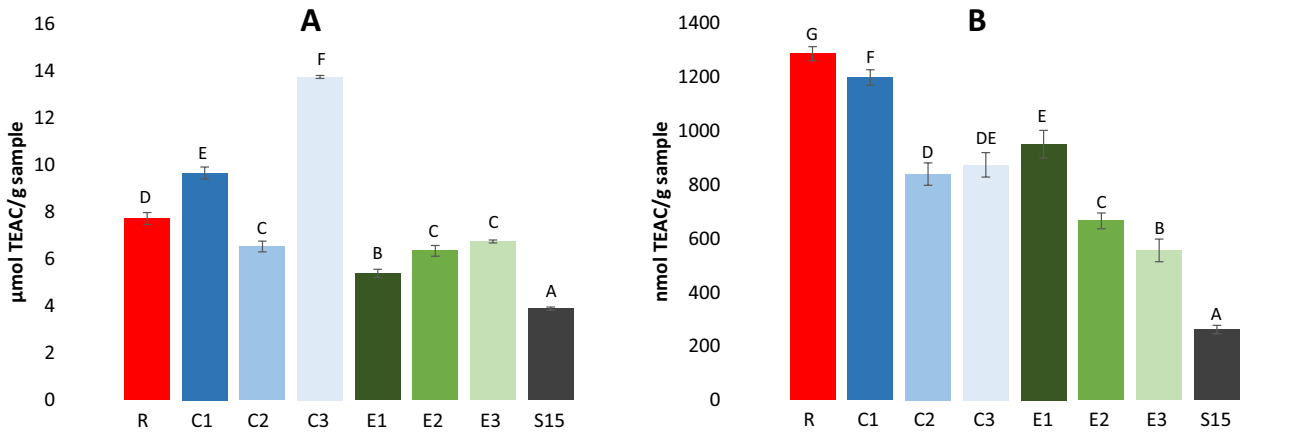

Fig. 7 DPPH radical scavenging activity (**A**) and ABTS radical scavenging activity (**B**) of the raw (R, red bar), control (C, blue bars), enzyme-treated (E, green bars) samples for the three different process phases and of the 15-min steamed samples (S15, dark gray bar) with standard deviation. Uppercase letters indicate significant differences among all the samples

metabolites like those described by Dini et al. (2013). This cooking effect has also been reported by Paciulli et al. (2019) when investigating the effect of heat treatment for 5 min on pumpkins' antioxidant activity measured by the DPPH assay. Despite this increased antioxidant activity not being observed in E3, these samples showed 42% greater activity than the S15 samples.

The ABTS method showed the greatest antioxidant capacity for the R samples (1287.9 ± 25.7 nmol TEAC/g), whereas the antioxidant activity of samples C and E significantly decreased after the vacuum treatment phase (6.9% and 26.1% for C1 and E1, respectively) (Fig. 7B). The ABTS values of samples C and E lowered (by around 30%) after the enzyme action phase, and activity additionally decreased in the E3 samples. This means that the antioxidant capacity of the E3 samples was significantly lesser than for the C3 samples. This behavior could be due to the possible leaching of hydrophilic antioxidant compounds as a consequence of a deteriorated structure and the greater extent of cell detachment that results from enzyme action, as observed in the previous section ("Stage 1: Effectiveness of the Enzyme Impregnation and Inactivation Treatments"). Nevertheless, the antioxidant capacity of E3 (556.7 ± 42.1 nmol TEAC/g sample) was significantly greater than that of S15, which had the lowest activity (262.5 ± 16.1 nmol TEAC/g sample). This was probably due to the aforementioned extensive cooking effect and to the increased bioaccessibility of the antioxidant compounds after enzyme action.

Sugar Determination

The total and reducing sugars contents were measured (Fig. 8) to explore the breakdown of pumpkin polysaccharides during processes (Yu et al., 2021). Similar profiles in the total and reducing sugar contents were observed for each pumpkin sample type. The total and reducing sugars contents increased for the C samples after the phase 3 (Fig. 8A and B, respectively), but non-significant differences were found with R and S15 in the former case. As expected, the reducing sugar content in C3 were lower than those of S15 because cooking normally increases sugar content (Bai et al., 2020; Singh et al., 2020). Regarding the E samples, the sugar content in E1 significantly lowered compared to R, but then they underwent a significant and noticeable increase in E2, followed by a sharp drop in E3, mainly for the reducing sugar content. At the end of the process, E3 were the samples with the lowest total and reducing sugar contents. The notorious sugar increase after the enzyme action time was probably due to a rise in the bioaccessibility of sugars as a result of enzyme action on pectin from cell walls. This action is based on the combination of PME and PG activities. While PME deesterifies pectin by producing methanol and peptic acid with a lower DE, PG hydrolyzes glycosidic bonds α-D-(1–4) in peptic acid (Fachin et al., 2003). The lower DE is, the higher the galactose concentration, and the lower GalA is (Zhemerichkin & Ptitchkina, 1995). Accordingly, the GalA concentrations of E3 and S15 were measured to evaluate the DE produced by enzyme action on pectin. The E3 samples had a lower GalA content (39.7 ± 3.3 mg GalA/g) than the S15 samples (49.9 ± 1.3 mg GalA/g), although differences were not significant. This suggests that E3 had a lower DE and higher galactose content than S15. This assumed increase in galactose concentration, which is a reducing sugar, could explain the higher reducing sugars content in relation to the total sugars content for E2. So the lower values of the sugars in E3 could be provoked by several effects. On the one hand, this could be due to a leaching effect and the release of a small part of sugars after the enzyme inactivation treatment which resulted from the unstructured enzyme-treated samples. On the other hand,

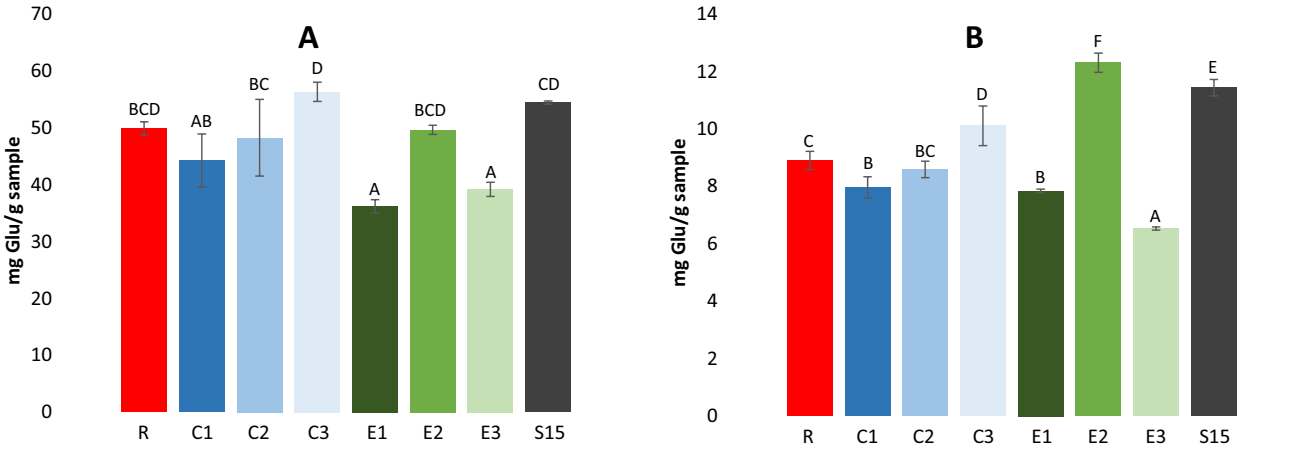

Fig. 8 Concentration of total (**A**) and reducing (**B**) sugars of the raw (R, red bar), control (C, blue bars) and enzyme-treated (E, green bars) samples for the three different process phases and of the 15-min steamed samples (S15, dark gray bar) with standard deviation. Uppercase letters indicate significant differences in all the samples

galactose could be isomerized to other monosaccharides with a lower glycemic index like tagatose due to the short heat treatment during which 85 °C was reached (Drabo & Delidovich, 2018). Tagatose is a rare ketohexose of much industrial interest for its low glycemic index and calorie value, and its good sweetening properties (Bober & Nair, 2019). Thus, the E3 samples had significantly lower total and reducing sugars contents than S15 (Fig. 8).

Our overall results make the enzyme-treated samples an interesting TM food for the elderly population, which tends to have many chewing and swallowing difficulties and major texture restrictions. These pumpkins offer improved texture properties for this population. Furthermore, the combined effects of enzyme hydrolysis action and the reduced heat treatment needed for softening allowed us to obtain a TM pumpkin with greater antioxidant activity and a lower sugar content than traditionally cooked pumpkins (S15). As discussed above, increased antioxidant activity can provide benefits by counteracting oxidative stress (Achir et al., 2016; Lee et al., 2020; Wichansawakun et al., 2022), whereas lower sugar content can be an advantage for the elderly because of low total energy use (Segura-Badilla et al., 2018).

Conclusions

TM pumpkin with suitable texture properties for people with swallowing and chewing difficulties, such as the elderly, was achieved. The enzyme-softened samples reached texture levels of strength and stiffness (no fracture point; Young's modulus: 181.7 ± 126.0 kPa) that are impossible with traditional cooking (fracture point: 6.6 ± 2.6 N; Young's modulus: 309.8 ± 69.7 kPa), achieving a homogeneous texture profile and maintaining their original appearance, which makes this TM food a more appealing alternative than mashed foods, such as purées or creams. The LLBI data demonstrated the feasibility of the enzyme impregnation process and the efficacy of the inactivation conditions by the short heat treatment, as no changes in light intensity occurred which would have expressed changes in the structure. The microscopic assay permitted us to observe the destruction of the cell walls because of the enzyme action. The kinetic of the reaction to degrade the pectin was observed by image segmentation. Furthermore, the effect of enzyme treatment on both antioxidant capacity and sugar content was evaluated and compared to traditionally cooked pumpkins and showed greater antioxidant capacity (ABTS: 52% higher; DPPH: 42% higher) and lower sugar content than the cooked pumpkins (total sugars: 29% lower). The overall results of this study make the TM pumpkins a suitable food for the elderly population with swallowing and chewing difficulties and provide valuable information about nutritional effects because of enzyme action effects. However, further studies on the specific compounds responsible for the observed antioxidant activities, monosaccharides composition, and digestibility are required to improve the quality and optimization of the TM foods designed for specific elderly populations. Moreover, it would be interesting to carry out a sensory analysis with this population to evaluate the sensory acceptance of the end product.

Author Contribution SH: Conceptualization, methodology, investigation, visualization, writing—original draft. MG: Conceptualization, methodology, investigation, visualization, writing—original draft. SV: Investigation, visualization, writing—original draft. JMB: Writing—review and editing. PT: Conceptualization; methodology; investigation; writing, review and editing; project administration; funding acquisition. RG: Conceptualization, methodology; investigation; resources; writing, original draft; supervision, project administration; funding acquisition.

Funding Open Access funding provided thanks to the CRUE-CSIC agreement with Springer Nature. Grant RTI2018-098842-B-I00 funded by MCIN/AEI/1013039/501100011033 and by ERDF "A way of making Europe" is acknowledged. M.G. gratefully acknowledges the Universitat Politècnica de València for her Postdoctoral grant (PAID-10–19).

Data Availability The data used in this study are available from the corresponding author upon reasonable request.

Declarations

Competing Interests The authors declare no competing interests.

References

Achir, N., Dhuique-Mayer, C., Hadjal, T., Madani, K., Pain, J. P., & Dornier, M. (2016). Pasteurization of citrus juices with ohmic heating to preserve the carotenoid profile. *Innovative Food Science and Emerging Technologies, 33*, 397–404. https://doi.org/10.1016/j.ifset.2015.11.002

Adebayo, S. E., Hashim, N., Abdan, K., & Hanafi, M. (2016). Application and potential of backscattering imaging techniques in agricultural and food processing - A review. *Journal of Food Engineering, 169*, 155–164. https://doi.org/10.1016/j.jfoodeng.2015.08.006

Aguilera, J. M., & Park, D. J. (2016). Texture-modified foods for the elderly: Status, technology and opportunities. *Trends in Food Science and Technology, 57*, 156–164. https://doi.org/10.1016/j.tifs.2016.10.001

Alcalde, S., Ricote, M., & Rodríguez, R. (2020). Dysphagia Guide. Feeding in dysphagia: textural adequacy and the use of thickeners (Chapter 7).

Andersson, J., Garrido-Bañuelos, G., Bergdoll, M., Vilaplana, F., Menzel, C., Mihnea, M., & Lopez-Sanchez, P. (2022). Comparison of steaming and boiling of root vegetables for enhancing carbohydrate content and sensory profile. *Journal of Food Engineering*, *312*. https://doi.org/10.1016/j.jfoodeng.2021.110754

Bai, Y., Zhang, M., Chandra Atluri, S., Chen, J., & Gilbert, R. G. (2020). Relations between digestibility and structures of pumpkin starches and pectins. *Food Hydrocolloids*, *106*. https://doi.org/10.1016/j.foodhyd.2020.105894

Bermejo-Prada, A., van Buggenhout, S., Otero, L., Houben, K., van Loey, A., & Hendrickx, M. E. (2014). Kinetics of thermal and high-pressure inactivation of avocado polygalacturonase. *Innovative Food Science and Emerging Technologies, 26*, 51–58. https://doi.org/10.1016/j.ifset.2014.05.005

Bober, J. R., & Nair, N. U. (2019). Galactose to tagatose isomerization at moderate temperatures with high conversion and productivity. *Nature Communications*, *10*(1). https://doi.org/10.1038/s41467-019-12497-8

Cesaretti, M., Luppi, E., Maccari, F., & Volpi, N. (2003). A 96-well assay for uronic acid carbazole reaction. *Carbohydrate Polymers, 54*(1), 59–61. https://doi.org/10.1016/S0144-8617(03)00144-9

Cichero, J. A. Y., Steele, C., Duivestein, J., Clavé, P., Chen, J., Kayashita, J., Dantas, R., Lecko, C., Speyer, R., Lam, P., & Murray, J. (2013). The need for international terminology and definitions for texture-modified foods and thickened liquids used in dysphagia management: Foundations of a global initiative. *Current Physical Medicine and Rehabilitation Reports, 1*(4), 280–291. https://doi.org/10.1007/s40141-013-0024-z

Dini, I., Tenore, G. C., & Dini, A. (2013). Effect of industrial and domestic processing on antioxidant properties of pumpkin pulp. *LWT - Food Science and Technology, 53*(1), 382–385. https://doi.org/10.1016/j.lwt.2013.01.005

Drabo, P., & Delidovich, I. (2018). Catalytic isomerization of galactose into tagatose in the presence of bases and Lewis acids. *Catalysis Communications, 107*, 24–28. https://doi.org/10.1016/j.catcom.2018.01.011

Dubois, M., Gilles, K. A., Hamilton, J. K., Rebers, P. A., & Smith, F. (1956). Colorimetric method for determination of sugars and related substances. *Analytical Chemistry, 28*(3), 350–356. https://doi.org/10.1021/ac60111a017

Eom, S. H., Chun, Y. G., Park, C. E., Kim, B. K., Lee, S. H., & Park, D. J. (2018). Application of freeze–thaw enzyme impregnation to produce softened root vegetable foods for elderly consumers. *Journal of Texture Studies, 49*(4), 404–414. https://doi.org/10.1111/jtxs.12341

Fachin, D., van Loey, A. M., Ly Nguyen, B., Verlent, I., Indrawati, A., & Hendrickx, M. E. (2003). Inactivation kinetics of polygalacturonase in tomato juice. *Innovative Food Science and Emerging Technologies, 4*(2), 135–142. https://doi.org/10.1016/S1466-8564(02)00090-5

Fuentes, C., Verdú, S., Fuentes, A., Ruiz, M. J., & Barat, J. M. (2022). Effects of essential oil components exposure on biological parameters of Caenorhabditis elegans. *Food and Chemical Toxicology*, *159*. https://doi.org/10.1016/j.fct.2021.112763

Gallego, M., Arnal, M., Barat, J. M., & Talens, P. (2021). Effect of cooking on protein digestion and antioxidant activity of different legume pastes. *Foods, 10*(1). https://doi.org/10.3390/foods10010047

Gallego, M., Barat, J. M., Grau, R., & Talens, P. (2022). Compositional, structural design and nutritional aspects of texture-modified foods for the elderly. *Trends in Food Science and Technology, 119*, 152–163. https://doi.org/10.1016/j.tifs.2021.12.008

Grau, R., Verdú, S., Pérez, A. J., Barat, J. M., & Talens, P. (2021). Laser-backscattering imaging for characterizing pork loin tenderness. Effect of pre-treatment with enzyme and cooking. *Journal of Food Engineering*, *299*. https://doi.org/10.1016/j.jfoodeng.2021.110508

Gwala, S., Wainana, I., Pallares Pallares, A., Kyomugasho, C., Hendrickx, M., & Grauwet, T. (2019). Texture and interlinked post-process microstructures determine the in vitro starch digestibility of Bambara groundnuts with distinct hard-to-cook levels. *Food Research International, 120*, 1–11. https://doi.org/10.1016/j.foodres.2019.02.022

Huang, D., Boxin, O. U., & Prior, R. L. (2005). The chemistry behind antioxidant capacity assays. *Journal of Agricultural and Food Chemistry, 53*(6), 1841–1856. https://doi.org/10.1021/jf030723c

Kao, F. J., Chiu, Y. S., & Chiang, W. D. (2014). Effect of water cooking on antioxidant capacity of carotenoid-rich vegetables in Taiwan. *Journal of Food and Drug Analysis, 22*(2), 202–209. https://doi.org/10.1016/j.jfda.2013.09.010

Lee, S. F., Harris, R., & Stout-Delgado, H. W. (2020). Targeted antioxidants as therapeutics for treatment of pneumonia in the elderly. *Translational Research, 220*, 43–56. https://doi.org/10.1016/j.trsl.2020.03.002

Lešková, E., Kubíková, J., Kováčiková, E., Košická, M., Porubská, J., & Holčíková, K. (2006). Vitamin losses: Retention during heat treatment and continual changes expressed by mathematical models. *Journal of Food Composition and Analysis, 19*(4), 252–276. https://doi.org/10.1016/j.jfca.2005.04.014

Li, F., Wei, Y., Liang, L., Huang, L., Yu, G., & Li, Q. (2021). A novel low-molecular-mass pumpkin polysaccharide: Structural characterization, antioxidant activity, and hypoglycemic potential. *Carbohydrate Polymers*, *251*. https://doi.org/10.1016/j.carbpol.2020.117090

Longato, E., Lucas-González, R., Peiretti, P. G., Meineri, G., Pérez-Alvarez, J. A., Viuda-Martos, M., & Fernández-López, J. (2017). The effect of natural ingredients (amaranth and pumpkin seeds) on the quality properties of chicken burgers. *Food and Bioprocess Technology, 10*(11), 2060–2068. https://doi.org/10.1007/s11947-017-1978-0

Lyu, Y., Bi, J., Chen, Q., Wu, X., Qiao, Y., Hou, H., & Zhang, X. (2021). Bioaccessibility of carotenoids and antioxidant capacity of seed-used pumpkin byproducts powders as affected by particle size and corn oil during in vitro digestion process. *Food Chemistry, 343*. https://doi.org/10.1016/j.foodchem.2020.128541

Mashiane, P., Mashitoa, F. M., Slabbert, R. M., & Sivakumar, D. (2021). Impact of household cooking techniques on colour, antioxidant and sensory properties of African pumpkin and pumpkin leaves. *International Journal of Gastronomy and Food Science*, *23*. https://doi.org/10.1016/j.ijgfs.2021.100307

Medina-Torres, L., Calderas, F., Gallegos-Infante, J. A., Gonzalez-Laredo, R. F., Rocha-Guzman, N. E., & Harte, F. (2009). Mechanical properties of ovalbumin gels formed at different conditions of concentration, ionic strength, pH, and aging time. *Food and Bioprocess Technology, 3*(1), 150–154. https://doi.org/10.1007/s11947-009-0257-0

Miglio, C., Chiavaro, E., Visconti, A., Fogliano, V., & Pellegrini, N. (2008). Effects of different cooking methods on nutritional and physicochemical characteristics of selected vegetables. *Journal of Agricultural and Food Chemistry, 56*(1), 139–147. https://doi.org/10.1021/jf072304b

Nakatsu, S., Kohyama, K., Watanabe, Y., Shibata, K., Sakamoto, K., & Shimoda, M. (2012). Mechanical properties of softened foodstuffs processed by freeze-thaw infusion of macerating enzyme. *Innovative Food Science and Emerging Technologies, 16*, 267–276. https://doi.org/10.1016/j.ifset.2012.07.010

Paciulli, M., Rinaldi, M., Rodolfi, M., Ganino, T., Morbarigazzi, M., & Chiavaro, E. (2019). Effects of high hydrostatic pressure on physico-chemical and structural properties of two pumpkin species. *Food Chemistry, 274*, 281–290. https://doi.org/10.1016/j.foodchem.2018.09.021

Park, J. J., & Lee, W. Y. (2020). Softening of lotus root and carrot using freeze-thaw enzyme infusion for texture-modified foods. *Food Bioscience*, *35*. https://doi.org/10.1016/j.fbio.2020.100557

Phuhongsung, P., Zhang, M., & Devahastin, S. (2020). Influence of surface pH on color, texture and flavor of 3D printed composite mixture of soy protein isolate, pumpkin, and beetroot. *Food and Bioprocess Technology, 13*(9), 1600–1610. https://doi.org/10.1007/s11947-020-02497-8

Prior, R. L., Wu, X., & Schaich, K. (2005). Standardized methods for the determination of antioxidant capacity and phenolics in foods and dietary supplements. *Journal of Agricultural and Food Chemistry, 53*(10), 4290–4302. https://doi.org/10.1021/jf0502698

Ribeiro, E. M. G., Chitchumroonchokchai, C., de Carvalho, L. M. J., de Moura, F. F., de Carvalho, J. L. V., & Failla, M. L. (2015). Effect of style of home cooking on retention and bioaccessibility of pro-vitamin A carotenoids in biofortified pumpkin (*Cucurbita moschata Duch.*). *Food Research International, 77*, 620–626. https://doi.org/10.1016/j.foodres.2015.08.038

Roininen, K., Fillion, L., Kilcast, D., & Lähteenmäki, L. (2004). Exploring difficult textural properties of fruit and vegetables for the elderly in Finland and the United Kingdom. *Food Quality and Preference, 15*(6), 517–530. https://doi.org/10.1016/j.foodqual.2003.11.003

Sakamoto, K., Shibata, K., & Ishihara, M. (2006). Decreased hardness of dietary fiber-rich foods by the enzyme-infusion method. *Bioscience, Biotechnology and Biochemistry, 70*(7), 1564–1570. https://doi.org/10.1271/bbb.50562

Segura-Badilla, O., Kammar-García, A., Vera-López, O., Aguilar-Alonso, P., Lazcano-Hernández, M., Avila-Sosa, R., & Navarro-Cruz, A. R. (2018). Simplified equation for resting energy expenditure in a population of elderly Chileans compared to indirect calorimetry. *NFS Journal, 13*, 23–29. https://doi.org/10.1016/j.nfs.2018.10.002

Shibata, K., Sakamoto, K., Ishihara, M., Nakatsu, S., Kajihara, R., & Shimoda, M. (2010). Effects of freezing conditions on enzyme impregnation into food materials by freeze-thaw infusion. *Food Science and Technology Research, 16*(5), 359–364. https://doi.org/10.3136/fstr.16.359

Singh, A., Raigond, P., Lal, M. K., Singh, B., Thakur, N., Changan, S. S., Kumar, D., & Dutt, S. (2020). Effect of cooking methods on glycemic index and in vitro bioaccessibility of potato (Solanum tuberosum L.) carbohydrates. *LWT*, *127*. https://doi.org/10.1016/j.lwt.2020.109363

Su, D., Wang, Z., Dong, L., Huang, F., Zhang, R., Jia, X., Wu, G., & Zhang, M. (2019). Impact of thermal processing and storage temperature on the phenolic profile and antioxidant activity of different varieties of lychee juice. *LWT*, *116*. https://doi.org/10.1016/j.lwt.2019.108578

Sun, J., Zhou, W., Huang, D., Fuh, J. Y. H., & Hong, G. S. (2015). An overview of 3D printing technologies for food fabrication. *Food and Bioprocess Technology, 8*(8), 1605–1615. https://doi.org/10.1007/s11947-015-1528-6

Tomašević, I., Putnik, P., Valjak, F., Pavlić, B., Šojić, B., Bebek Markovinović, A., & Bursać Kovačević, D. (2021). 3D printing as novel tool for fruit-based functional food production. *Current Opinion in Food Science, 41*, 138–145. https://doi.org/10.1016/j.cofs.2021.03.015

United Nations. (2020). Department of economic and social affairs, population division. World Population Ageing 2020 Highlights: Living arrangements of older persons. ST/ESA/SER.A/451.

Verdú, S., Barat, J. M., & Grau, R. (2019). Laser backscattering imaging as a non-destructive quality control technique for solid food matrices: Modelling the fibre enrichment effects on the physico-chemical and sensory properties of biscuits. *Food Control, 100*, 278–286. https://doi.org/10.1016/j.foodcont.2019.02.004

Verdú, S., Pérez, A. J., Barat, J. M., & Grau, R. (2021). Non-destructive control in cheese processing: Modelling texture evolution in the milk curdling phase by laser backscattering imaging. *Food Control*, *121*. https://doi.org/10.1016/j.foodcont.2020.107638

Wichansawakun, S., Chupisanyarote, K., Wongpipathpong, W., Kaur, G., & Buttar, H. S. (2022). Antioxidant diets and functional foods attenuate dementia and cognition in elderly subjects. *Functional Foods and Nutraceuticals in Metabolic and Non-Communicable Diseases*, 533–549. https://doi.org/10.1016/b978-0-12-819815-5.00028-8

Wilson, A., Anukiruthika, T., Moses, J. A., & Anandharamakrishnan, C. (2020). Customized shapes for chicken meat–based products: Feasibility study on 3D-printed nuggets. *Food and Bioprocess Technology, 13*(11), 1968–1983. https://doi.org/10.1007/s11947-020-02537-3

Yang, H., Wu, Q., Ng, L. Y., & Wang, S. (2017). Effects of vacuum impregnation with calcium lactate and pectin methylesterase on

quality attributes and chelate-soluble pectin morphology of fresh-cut papayas. *Food and Bioprocess Technology, 10*(5), 901–913. https://doi.org/10.1007/s11947-017-1874-7

Yu, G., Zhao, J., Wei, Y., Huang, L., Li, F., Zhang, Y., & Li, Q. (2021). Physicochemical properties and antioxidant activity of pumpkin polysaccharide (*Cucurbita moschata Duchesne ex Poiret*) modified by subcritical water. https://doi.org/10.3390/foods1001

Zhemerichkin, D. A., & Ptitchkina, N. M. (1995). The composition and properties of pumpkin and sugar beet pectins. *Topics in Catalysis, 9*(2), 147–149. https://doi.org/10.1016/S0268-005X(09)80277-4

Zhou, C. L., Liu, W., Zhao, J., Yuan, C., Song, Y., Chen, D., Ni, Y. Y., & Li, Q. H. (2014). The effect of high hydrostatic pressure on the microbiological quality and physical-chemical characteristics of pumpkin (Cucurbita maxima Duch.) during refrigerated storage. *Innovative Food Science and Emerging Technologies, 21*, 24–34. https://doi.org/10.1016/j.ifset.2013.11.002

Zhou, C. L., Mi, L., Hu, X. Y., & Zhu, B. H. (2017). Evaluation of three pumpkin species: Correlation with physicochemical, antioxidant properties and classification using SPME-GC–MS and E-nose methods. *Journal of Food Science and Technology, 54*(10), 3118–3131. https://doi.org/10.1007/s13197-017-2748-8